2014 American Control Conference (ACC)
June 4-6, 2014. Portland, Oregon, USA

Nonlinear Observer Designs for State-of-Charge Estimation of Lithium-ion Batteries

Satadru Dey and Beshah Ayalew

Abstract—**State-of-Charge (SOC) information is very crucial for the control, diagnostics and monitoring of Li-ion cells/batteries. Compared to conventional data-driven or equivalent circuit models often employed in battery management systems, electrochemical battery models have the potential to give physically accurate the SOC information by tracking the Li-ion concentration in each electrode. In this paper, two nonlinear observer designs are presented to estimate Li-ion battery State-of-Charge based on reductions of an electrochemical model. The first observer design uses a constant gain Luenberger structure whereas the second one improves it by weighing the gain with the output Jacobian. For both observer designs, Lyapunov's direct method is applied and the design problems are converted to solving LMIs. Simulation results are included to demonstrate the effectiveness of both observer designs.**

I. Introduction

Electrified vehicles are predicted to take increasing shares in the vehicle market in the near future because of their reduced on-board emissions and improved energy efficiency benefits [1, 2]. Lithium-ion (Li-ion) batteries have been gaining substantial interest in these vehicles and many other applications due to their high energy density, negligible self-discharge and less environmental impact. However, advanced Battery Management Systems (BMS) with precise knowledge of State-of-Charge (SOC) are essential for safe and efficient operation of Li-ion batteries. In this paper, we will concentrate on SOC estimation for an individual Li-ion battery cell.

In current literature, various SOC estimation algorithms exist, which can be broadly categorized into two groups: model-free approaches such as coulomb-counting, Open Circuit Voltage (OCV) vs. SOC maps [3] and model-based approaches. Model-free approaches are easy to implement but prone to measurement errors and inaccuracy. Model-based approaches can be divided into three categories depending on the source of the model: data-driven model, equivalent circuit model (ECM) and electrochemical model. Data-driven approaches derive models from measurement data [4]. ECM-based approaches use an electric circuit model to mimic the battery behavior [5, 6 and 7]. Although these approaches are simple in implementation, the drawbacks are requirement of extensive parameterization and the lack of physical information about the battery.

Electrochemical model-based approaches rely on a physical model derived from porous electrode and concentrated solution theories. In the current literature, there are two broad classes of electrochemical model-based SOC estimators. The first class utilizes the so-called pseudo-two-dimensional (P2D) full order battery cell model [16, 17] directly. A particle filtering framework based on this model has been proposed in [14]. However, the computational burden is high in real-time implementation of such estimators. Another work [15] proposed a Luenberger-type observer for the P2D model but the stability properties of the observer were not analyzed fully, possibly due to the complexity of the model.

The second class of electrochemical model-based estimators reduces the model complexity by simplifying the P2D model by approximating both electrodes as single spherical particles (generally referred to as the Single Particle Model (SPM)). A PDE estimator has been designed based on SPM in [8]. In some other works, an ODE approximation of this SPM PDEs has been considered for estimator design. A reduced linearized model with a Kalman filter has been used in [9, 10]. Some approaches apply the Extended Kalman Filter (EKF) on some ODE versions of the SPM [11, 13]. The downside is that EKF does not provide an optimal estimate and high initial state errors may lead to divergence owing to internal linearization. In addition, for higher dimensional approximations, the computational burden can be high for EKF. The SPM model was extended in [12] adding electrolyte dynamics followed by designing an Unscented Kalman Filter (UKF). However, the computational complexity of UKF can also be high for real-time implementation. Despite good performance, one of the drawbacks of EKF/UKF is that the sufficient conditions [21] for the convergence or boundedness of the estimation error are in reality difficult to impose or verify [22].

From the above review on electrochemical model-based SOC estimators, it can be concluded that most of the existing work has one or more of the following issues: 1) utilizes a fully linearized model, 2) computationally expensive, and 3) lacks theoretical verification of the convergence of the estimation error. In this paper, two nonlinear observer designs have been proposed which address the above issues. These observers utilize an ODE approximation of the SPM where the observer design boils down to solving a Linear Matrix Inequality (LMI) problem. The design process preserves the essential output nonlinearity of the system, and

*Research supported by U.S. Department of Energy's GATE Program.

S. Dey is with Clemson University International Center for Automotive Research, Greenville, SC 29607 USA (Corresponding author: phone: 864-908-4336; fax: 864-283-7208; e-mail: satadrd@clemson.edu).

B. Ayalew is with Clemson University International Center for Automotive Research, Greenville, SC 29607 USA (e-mail: beshah@clemson.edu).

once the observers are designed, the implementation has a very low computational burden. The asymptotic convergence of the estimation error can be guaranteed theoretically using Lyapunov's direct method. The performance of the observers is demonstrated by applying the observers on the SPM and P2D models of a Li-ion battery cell.

The rest of the paper is organized as follows. Section II reviews the Li-ion battery cell model adopted for this study, Section III outlines the details of the two nonlinear observer designs, and Section IV presents results and discussions. Section V summarizes the conclusions of the work.

II. Lithium-ion Battery Cell Model

Full order battery cell P2D electrochemical model [10, 16 and 17] contains accurate physical information of the battery internal dynamics. However, it is computationally expensive for real-time implementation. Therefore, a reduced version of the P2D model, Single Particle Model (SPM) that approximates the electrodes as spherical particles is considered [11, 13]. This assumption leads to two linear solid-state diffusion PDEs given by (1), with a nonlinear output voltage map given by (2), which is derived from Bulter-Volmer kinetics. In this framework, the bulk SOC is directly related to the summation of Li-ion concentrations along the radius of the spherical particle.

$$\frac{\partial c_s^{\pm}}{\partial t} = \frac{D_s^{\pm}}{r^2}\frac{\partial}{\partial r}\left(r^2\frac{\partial c_s^{\pm}}{\partial r}\right)$$
$$\left.\frac{\partial c_s^{\pm}}{\partial r}\right|_{r=0} = 0, \qquad \left.\frac{\partial c_s^{\pm}}{\partial r}\right|_{r=R} = \frac{\pm I}{a_s^{\pm} F D_s^{\pm} A L^{\pm}} \tag{1}$$

$$V = \frac{\bar{R}T}{\alpha^{+}F}\sinh^{-1}\left(\frac{I}{2a_s^{+}AL^{+}\sqrt{c_e c_{s,e}^{+}\left(c_{s,max}^{+} - c_{s,e}^{+}\right)}}\right)$$
$$-\frac{\bar{R}T}{\alpha^{-}F}\sinh^{-1}\left(\frac{I}{2a_s^{-}AL^{-}\sqrt{c_e c_{s,e}^{-}\left(c_{s,max}^{-} - c_{s,e}^{-}\right)}}\right)$$
$$+U^{+}\left(c_{s,e}^{+}\right) - U^{-}\left(c_{s,e}^{-}\right) - R_f I \tag{2}$$

where $c_s^{\pm}$ is the Li-ion concentration of the positive and negative electrode, V is the cell-voltage and I is the charge/discharge current. For definitions of the rest of the variables, the reader may refer to Table I.

As discussed in [13], in this SPM, the states are weakly observable from the voltage output. As a remedy to this problem, the approach in [8] is followed, where the positive electrode diffusion dynamics is assumed to have an algebraic relationship with that in the negative electrode. The physical reason behind this assumption, as also noted in [8], is the faster diffusion dynamics in the positive electrode compared to that of the negative electrode. This assumption reduces the model to a single PDE governing the dynamics in the negative electrode, which is strongly observable from the output. The local observability of this reduced model can be easily verified using model linearization at different operating points.

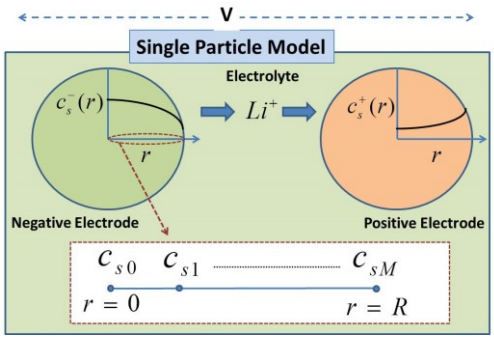

Figure 1. Schematic of Single Particle Model

TABLE I: Li-ion battery model nomenclature

Symbol	Definition and Unit
A	Current collector area (cm^2)
$a_s^{\pm}$	Specific surface area (cm^2/cm^3)
c_e	Electrolyte phase Li-ion concentration (mol/cm^3)
$c_s^{\pm}$	Solid phase Li-ion concentration (mol/cm^3)
$c_{s,e}^{\pm}$	Solid phase Li-ion concentration at surface (mol/cm^3)
$c_{s,max}^{\pm}$	Solid phase Li-ion saturation concentration (mol/cm^3)
$D_s^{\pm}$	Effective diffusion coefficient in solid phase (cm^2/s)
F	Faraday's constant (C/mol)
I	Current (A)
$L^{\pm}$	Length of the cell (cm)
r	Radial coordinate (cm)
R	Radius of solid active particle (cm)
$\bar{R}$	Universal Gas Constant (J/mol-K)
R_f	Contact film resistance (Ω)
T	Temperature (K)
$U^{\pm}$	Open circuit potential (V)
$\alpha^{\pm}$	Charge transfer coefficient
Superscript	
$\pm$	positive/negative electrode

To approximate the PDE in (1), the method of lines technique is used where the spatial derivatives are discretized using finite difference methods. This leads to a set of ODEs that form the finite dimensional state-space model of the battery cell. The central difference formula is used along with the imaginary node concept. The spatial domain is discretized into (M+1) nodes. The $[c_{s0}, c_{s1}, \ldots c_{sM}]$ are the Li-ion concentration states at the nodes; c_{s0} is the concentration of the center node of the particle and c_{sM} is the concentration of the surface node of the particle. An illustration of SPM along with the finite difference discretization adopted is given in Fig. 1. The resulting ODEs are given in (3).

$$\dot{c}_{s0} = -3ac_{s0} + 3ac_{s1}$$
$$\dot{c}_{sm} = \left(1 - \frac{1}{m}\right)ac_{s(m-1)} - 2ac_{sm} + \left(1 + \frac{1}{m}\right)ac_{s(m+1)}$$
$$\dot{c}_{sM} = \left(1 - \frac{1}{M}\right)ac_{s(M-1)} - \left(1 - \frac{1}{M}\right)ac_{sM} - \left(1 + \frac{1}{M}\right)bI \tag{3}$$

with $m = 1, \ldots, (M-1)$, discretization step $\Delta = R/M$, $a = D_s^{-}/\Delta^2$, $b = 1/a_s^{-}F\Delta AL^{-}$. It can be noted that model (3)

provides information about bulk SOC, which indicates total charge left in the cell, and surface SOC, which is an indicator of available power. Bulk SOC of the cell can be computed as $soc_{bulk} = \sum_{i=0}^{M} c_{si}$ whereas c_{sM} indicates the surface SOC. The voltage equation can be formed from (2) by substituting $c_{s,e}^{-} = c_{sM}$ and $c_{s,e}^{+} = k_1 c_{sM} + k_2$ where k_1 and k_2 are constants in the algebraic relationship between cathode and anode Li-ion concentration. These constants for model reduction can be derived based on conservation of total number of the Li-ions [8].

III. Nonlinear Observer Design

The above model (3) can be re-written in the state-space form:

$$\dot{x} = Ax + Bu$$
$$y = h(x, u) \tag{4}$$

where states $x = [c_{s1}, \dots, c_{sM}]^T \in R^M$, input current $u = I \in R$, output voltage $y = V \in R$, the matrices A and B are derived from (3) and the output function h is formed by (2) as discussed in previous section. It is observed that keeping the zero-th node dynamics in the state-space model leads to unobservability. As a remedy, the zero-th node dynamics is removed from the state-space model. This does not lead to any information loss as the zero-th node dynamics can be reconstructed using the estimated 1st node information. Finally, the problem at hand is to estimate the states of the system (4) which is described by linear dynamics with nonlinear output. The local observability of the system is verified at different operating points using the state-space model based on the A matrix and linearized output C matrix from the nonlinear output map in (4).

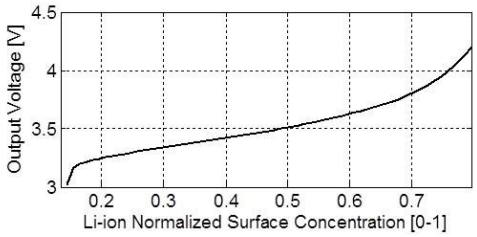

Figure 2. Output Voltage as a Function of State

The output function of the system is shown in Fig. 2 (with respect to c_{sM}, since the output is only a function of surface concentration of Li-ions) for some given input. It can be noted that the trend of the output function remains the same irrespective of the input value; only a voltage offset is added due to different resistive drops. It is clear that the output function is strictly increasing and continuously differentiable with respect to the state within the range of operation. The continuous differentiability property of the output function serves as a sufficient condition for Lipschitz continuity [18]. These observations will be exploited in the two designs below. An estimate of the Lipschitz constant can be found as the $\max\left(\left\|\frac{\partial h}{\partial x}\right\|\right)$ within the operating region. Practically, the Lipschitz constant for a Li-ion cell can be estimated from maximum slope of battery voltage vs. state-of-charge data usually given in datasheets.

A. Nonlinear Observer Design I: Constant Gain Observer

In this first design, the Luenberger observer structure (5) is chosen.

$$\dot{\hat{x}} = A\hat{x} + Bu + L(y - \hat{y})$$
$$\hat{y} = h(\hat{x}, u) \tag{5}$$

The constant observer gain L is to be designed. The estimator error dynamics is given as:

$$\dot{\tilde{x}} = \dot{x} - \dot{\hat{x}} = A\tilde{x} - z \tag{6}$$

where $z = L(y - \hat{y}) = L[h(x, u) - h(\hat{x}, u)]$

The previously mentioned Lipschitz continuity condition can be written as:

$$\|h(x, u) - h(\hat{x}, u)\| \le \gamma \|\tilde{x}\| \tag{7}$$

where γ is the Lipschitz's constant. Now, using Holder's inequality and Lipschitz continuity condition,

$$\|z\| \le \|L\| \|h(x, u) - h(\hat{x}, u)\|$$
$$\Rightarrow \|z\| \le \gamma \|L\| \|\tilde{x}\| \Rightarrow z^T z \le \gamma^2 L^T L \tilde{x}^T \tilde{x}$$

By adding a new (tuning) term, this condition can be modified as:

$$z^T z - \tilde{x}^T [(\gamma^2 L^T L) I] \tilde{x} \le -z^T M_1 z \tag{8}$$

where M_1 is some known positive definite matrix of the designer's choice and I is an identity matrix of appropriate dimension. The inequality (8) can be written as:

$$[\tilde{x}^T \quad z^T] \begin{bmatrix} (\gamma^2 L^T L) I & 0 \\ 0 & -I - M_1 \end{bmatrix} \begin{bmatrix} \tilde{x} \\ z \end{bmatrix} \ge 0 \tag{9}$$

Then, a Lyapunov function candidate $V = \tilde{x}^T P \tilde{x}$ is chosen to analyze the stability of the observer error dynamics where P is an unknown positive definite symmetric matrix. The derivative of the Lyapunov function candidate is given as:

$$\dot{V} = \tilde{x}^T [A^T P + PA] \tilde{x} - \tilde{x}^T P z - z^T P \tilde{x}$$

For $\dot{V}$ to be negative definite, the following condition should be satisfied,

$$-[\tilde{x}^T \quad z^T] \begin{bmatrix} A^T P + PA & -P \\ -P & 0 \end{bmatrix} \begin{bmatrix} \tilde{x} \\ z \end{bmatrix} > 0 \tag{10}$$

Therefore, for the observer dynamics of the given system to converge to zero asymptotically, the following LMIs must be satisfied for any suitable positive define M_1 of the designer's choice,

$$P > 0, -\begin{bmatrix} A^T P + PA & -P \\ -P & 0 \end{bmatrix} > 0,$$
$$\begin{bmatrix} (\gamma^2 L^T L) I & 0 \\ 0 & -I - M_1 \end{bmatrix} \ge 0 \tag{11}$$

Using the s-procedure [19], the 2nd and 3rd LMIs of (11) lead to the condition:

$$-\begin{bmatrix} A^T P + PA + (\tau \gamma^2 L^T L) I & -P \\ -P & -\tau (M_1 + I) \end{bmatrix} > 0$$

with some $\tau \ge 0$.

These LMIs can be solved using MATLAB's LMI Toolbox posing the problem in the following form:

$$\begin{bmatrix} A^TP + PA + Q & -P \\ -P & -SM \end{bmatrix} < 0; Q, S, P > 0 \quad (12)$$

where P is unknown symmetric positive definite matrix, $Q = qI$ (with scalar $q = (\tau\gamma^2 L^T L)$ as the element along the diagonal) and $S = sI$ (with scalar $s = \tau$ as the element along the diagonal) are unknown positive definite diagonal matrices with same elements along their diagonal, and $M(= M_1 + I > I)$ is a positive definite matrix of the designer's choice. Feasible solution of this LMI problem will result in negative definite $\dot{V}$, which guarantees asymptotic convergence of the estimation error in the absence of measurement noise and parametric/model uncertainty. The unknown observer gain vector can be solved for from the following:

$$L^T L = \frac{q}{s\gamma^2} \quad (13)$$

Note that (13) is only a condition on the sum of squares of observer gain vector elements. This provides an additional degree of freedom in choosing the individual elements of the gain vector.

With the above, we have established that the observer design can be consolidated as one of solving the LMIs (12). The tuning mechanisms of this design procedure are: the choice of M and choice of individual observer gain vector elements based on the condition (13). Different choices of these two will result in observers with different error convergence rates.

Systematic Gain Tuning Procedure:

1. The choice of M has to do with feasibility of the LMI problem (12) and the desired convergence rate. Choose the structure $M = \alpha I$. Initialize α with an arbitrary higher value greater than 1.
2. Start increasing α until a feasible LMI solution is achieved.
3. Once the LMI is feasible, record the value of $L^T L$ and repeat the procedure with further increasing α.
4. Finally, for all the feasible values of $L^T L$ assign the individual gain elements. Then select the observer gain L that gives the desired convergence rate.

B. *Nonlinear Observer Design II: Observer with Nonlinear Feedback*

The drawback of the constant gain observer described above is that it will feed the output error with the same amplification throughout the state trajectory. In some regions of the state space, where the sensitivity of the output with respect to the states is very low, constant gain tends to inject noise/disturbance without any useful information. Referring to Fig. 2, in the middle part of the state region the sensitivity of the output is very low. In this region, the constant gain could be disadvantageous. This fact motivates to have a gain-scheduled observer whose gain varies depending on the region of the state-space. In this design, the Jacobian of the output with respect to states is used to weigh the gain leading to the following structure [20]:

$$\dot{\hat{x}} = A\hat{x} + Bu + L\left[\frac{\partial h}{\partial x}\right]^T_{x=\hat{x}} (y - \hat{y})$$
$$\hat{y} = h(\hat{x}, u) \quad (14)$$

The error dynamics is given as:

$$\dot{\tilde{x}} = A\tilde{x} - L\left[\frac{\partial h}{\partial x}\right]^T_{x=\hat{x}} (h(x,u) - h(\hat{x},u)) \quad (15)$$

Again, a Lyapunov function candidate $V = \tilde{x}^T P \tilde{x}$ is chosen to analyze the convergence of the observer error dynamics, where P is an unknown positive definite symmetric matrix. The derivative of the Lyapunov function candidate is given as:

$$\dot{V} = \tilde{x}^T[A^TP + PA]\tilde{x} - 2\tilde{x}^T PL\left[\frac{\partial h}{\partial x}\right]^T \tilde{h} \quad (16)$$

where $\tilde{h} = h(x,u) - h(\hat{x},u)$ is the output error. Considering the first term of (16), the following condition is imposed to ensure the negative definiteness of the first term:

$$\tilde{x}^T[A^TP + PA]\tilde{x} \leq -\tilde{x}^T Q\tilde{x} - \tilde{x}^T PMP\tilde{x} \quad (17)$$

where Q and M are positive definite matrices of the designer's choice. The idea is to find a positive definite symmetric matrix P that satisfies (17). Assuming such P exists, the estimator gain matrix is chosen as $L = P^{-1}$. This choice of estimator gain matrix makes the 2nd term of (16) $2\tilde{x}^T\left[\frac{\partial h}{\partial x}\right]^T \tilde{h}$. Now, consider the fact that h is a strictly increasing function of only the end state ($x_M \triangleq c_{sM}$). This makes the x_M estimation error and output error sign always the same throughout the state trajectory. Also, the Jacobian $\frac{\partial h}{\partial x_M}$ is always positive in the operating region. The 2nd term on the right hand side of (16) can be written as:

$$2[\tilde{x}_1, \ldots, \tilde{x}_M]\left[0,0,\ldots,\frac{\partial h}{\partial x_M}\right]^T \tilde{h} = 2\tilde{x}_M \frac{\partial h}{\partial x_M}\tilde{h}$$

Now, $\tilde{x}_M\tilde{h} \geq 0$ at any point of the state space as the signs of $\tilde{x}_M$ and $\tilde{h}$ are always the same and $\frac{\partial h}{\partial x_M}$ is always positive (see Figure 2). This leads to the fact that $2\tilde{x}^T\left[\frac{\partial h}{\partial x}\right]^T \tilde{h} \geq 0$ at any point of the state space. Now, consider the derivative of the Lyapunov function candidate:

$$\dot{V} \leq -\tilde{x}^T Q\tilde{x} - \tilde{x}^T PMP\tilde{x} - 2\tilde{x}^T PL\left[\frac{\partial h}{\partial x}\right]^T \tilde{h}$$

It is clear that the first two terms are negative definite and the 3rd term is negative semi-definite. This leads to a negative definite $\dot{V}$ which is a sufficient condition for asymptotic convergence of observer error in the absence of measurement noise and parametric uncertainty. Therefore, the observer design boils down to finding a positive definite symmetric matrix P that satisfies (17). This can be cast as an LMI problem using Schur complements:

$$\begin{bmatrix} A^TP + PA + Q & P \\ P & -M^{-1} \end{bmatrix} < 0; P > 0 \quad (18)$$

Then the observer gain matrix can be obtained as $L = P^{-1}$. The tuning mechanisms for this design are the choices of Q and M; different combination of these will give different rates of convergence of the error.

Systematic Gain Tuning Procedure:

1. Similar to observer design I, the choice of Q and M has to do with feasibility of the LMI problem (18) and the desired convergence rate. Choose the structure $Q = \varepsilon_1 I$ and $M = \varepsilon_2 I$. Initialize $\varepsilon_1, \varepsilon_2 = 0$.
2. Start increasing ε_1 and ε_2 until a feasible LMI solution is achieved.
3. Once the LMI is feasible, record the gain L and repeat the procedure with further increasing ε_1 and ε_2.
4. Finally, from the set of feasible gains L, select the one that gives the desired error convergence rate.

IV. Results and Discussions

In this section, the performances of observers from the two designs are demonstrated via simulation studies. The observers are applied on both the SPM and P2D model of the Li-ion battery cell (as the plant). Model parameters of the Li-ion cell have been taken from [10]. To simulate realistic scenarios, noise of zero mean and 5 mV variance has been added to the measured voltage from the plant. Also, the observer has been initialized with a different value than the plant to evaluate its convergence. The input current profile used for simulation is: step of 30 A discharge from t = 0-25 sec, step of 30 A charge from t = 35-60 sec and zero current from t=25-35 sec. A 3rd order model (discretizing the particle radius into four nodes) has been used in the finite difference approximation.

In observer design I (with constant gain), the observer gain vector elements are chosen as $L^* = [0,0,\sqrt{L^T L}]$ where $\sqrt{L^T L} = 0.1$ for some choice of $M = diag(\alpha, \alpha, \alpha)$ with α as a high magnitude real number. Similarly, for Observer II (with nonlinear feedback), the observer gain matrix is found as:

$$L^* = \begin{bmatrix} 0.07 & 0.07 & 0.07 \\ 0.07 & 0.07 & 0.07 \\ 0.07 & 0.07 & 0.07 \end{bmatrix}$$

with choice $Q = diag(\varepsilon_1, \varepsilon_1, \varepsilon_1)$, $M = diag(\varepsilon_2, \varepsilon_2, \varepsilon_2)$ where $\varepsilon_1$and ε_2 as very small magnitude real numbers. At first, the observers' performances have been checked using SPM as the plant and utilizing the measurement from the same. The performance of the observers is shown in Fig. 3. In this illustration bulk Li-ion concentrations from observers and SPM have been used for comparison. It is clear from Fig. 3 that both observers I and II are able to track the states with sufficient accuracy. The observation error does not go to zero asymptotically because of the presence of noise in this illustration. However, the final steady-state error is within 0.05%, which is deemed satisfactory.

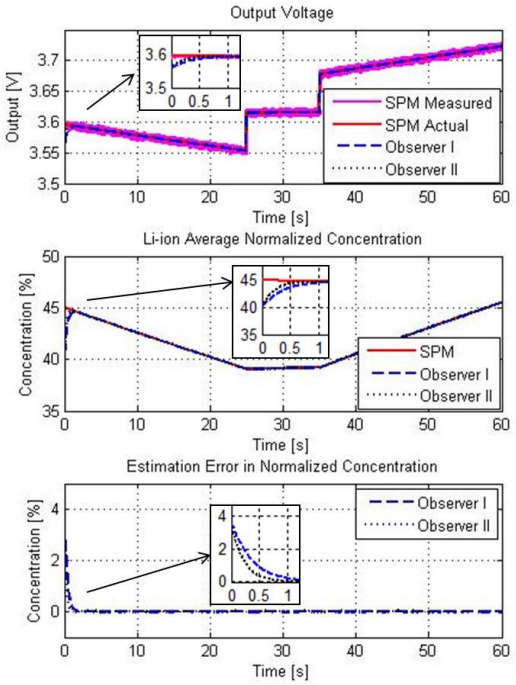

Figure 3. Performance of Observer I and II with SPM as Plant Model

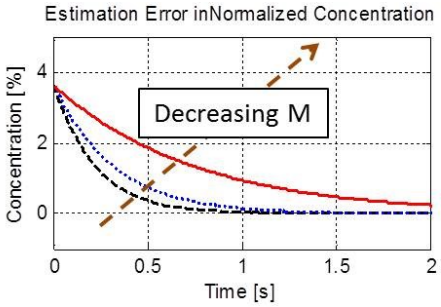

Figure 4. Error Convergence for Different Choices of the Tuning Parameter M

Note that the error convergence rates of the two observers are different due to the inherent difference in the selection of the tuning methods and parameters. The error convergence rate can be modified using the individual tuning mechanisms for the two observers as discussed in the design section. As an illustration, the error convergence rate of observer I is shown in Fig. 4 for different choices of the tuning parameter M. Similar modification can be done with observer II.

Next, the observers' performances have been checked using P2D model as the plant and utilizing the output measurement from the same. The performance is shown in Fig. 5. In this illustration, the averaged bulk concentration from the P2D model (i.e, the average of the concentrations at all spatial nodes along the length of the P2D cell) is compared with observer estimated bulk concentrations. As might be expected from the model mismatch between SPM and P2D, the estimation error is larger in this case. This is due to the fact that the system inherently acts as an integrator that causes the states to drift gradually under constant input. Owing to this integrator behavior, the mismatch between SPM and P2D models causes the error to not stabilize. However, the steady-state estimation error remains under 2%, which can also be deemed satisfactory.

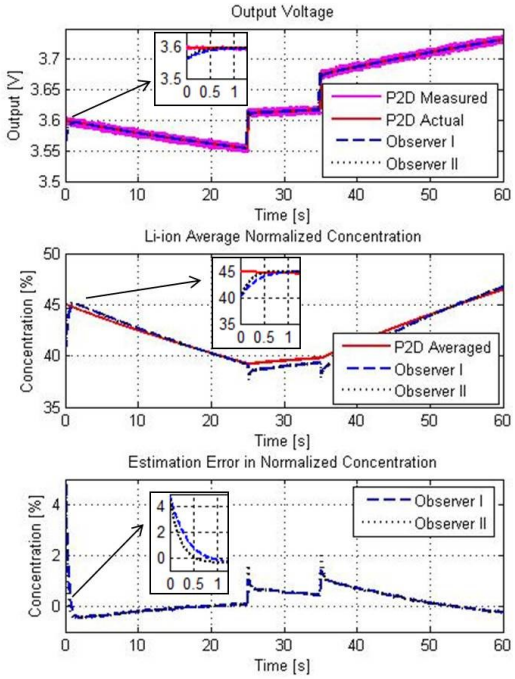

Figure 5. Performance of Observer I and II with P2D as Plant Model

V. CONCLUSION

In this paper, two nonlinear observer designs have been proposed for Li-ion battery cell SOC estimation. Both observers are developed based on finite difference ODE approximations of the so-called Single Particle Model (SPM). Observer I utilizes the Luenberger observer structure with constant gain whereas observer II improves the structure by weighing the gain with the Jacobian of the output with respect to states. Lyapunov's direct method has been applied to convert the estimator design problems into solving LMI problems. Tuning mechanisms have been added to both designs where the user has the freedom to modify some parameters to go for desired estimator error convergence rates. Simulation studies show that both estimators perform well even in the presence of measurement noise.

The proposed designs did not include parametric uncertainty in the model and also ignore the spatial variation of the battery variables. As future improvement of this current work, we plan to upgrade the observer design for a full order P2D model with parametric uncertainty.

REFERENCES

[1] D. Howell, "2010 Annual progress report for energy storage R&D," Vehicle Technologies Program, Energy Efficiency and Renewable Energy. U.S. Department of Energy, Washington, DC, 2011.

[2] A. G. Boulanger, A. C. Chu, S. Maxx, and D. L. Waltz, "Vehicle electrification: Status and issues," *Proceedings of the IEEE,* vol. 99, no. 6, pp. 1116-1138, 2011.

[3] S. Lee, J. Kim, J. Lee, and B. H. Cho, "State-of-charge and capacity estimation of lithium-ion battery using a new open-circuit voltage versus state-of-charge," *Journal of Power Sources,* vol. 185, no. 2, pp. 1367-1373, 2008.

[4] F. Sun, X. Hu, Y. Zou, and S. Li, "Adaptive unscented Kalman filtering for state of charge estimation of a lithium-ion battery for electric vehicles," *Energy*, vol. 36, no. 5, pp. 3531-3540, 2011.

[5] G. L. Plett, "Extended Kalman filtering for battery management systems of LiPB-based HEV battery packs: Part 3. State and parameter estimation," *Journal of Power sources,* vol. 134, no. 2, pp. 277-292, 2004.

[6] Y. Li, R. D. Anderson, J. Song, A. M. Phillips, and X. Wang, "A nonlinear adaptive observer approach for state of charge estimation of lithium-ion batteries," in *2011 American Control Conference (ACC)*, San Francisco, CA, USA, 2011.

[7] D. V. Do, C. Forgez, K. El-Kadri-Benkara, and G. Friedrich, "Impedance observer for a Li-ion battery using Kalman filter," *IEEE Transactions on Vehicular Technology*, vol. 58, no. 8, pp. 3930-3937, 2009.

[8] S. J. Moura, N. A. Chaturvedi, and M. Krstic, "PDE estimation techniques for advanced battery management systems—Part I: SOC estimation," in *2012 American Control Conference (ACC)*, pp. 559-565, 2012.

[9] K. A. Smith, C. D. Rahn, and C. Wang, "Model-based electrochemical estimation of lithium-ion batteries," in *IEEE 2008 International Conference on Control Applications*, pp. 714-719, 2008.

[10] K. A. Smith, C. D. Rahn, and C. Wang, "Model-based electrochemical estimation and constraint management for pulse operation of lithium ion batteries," *IEEE Transactions on Control Systems Technology*, vol. 18, no. 3, pp. 654-663, 2010.

[11] S. Santhanagopalan, and R. E. White, "Online estimation of the state of charge of a lithium ion cell," *Journal of Power Sources,* vol. 161, no. 2, pp. 1346-1355, 2006.

[12] S. Santhanagopalan, and R. E. White, "State of charge estimation using an unscented filter for high power lithium ion cells," *International Journal of Energy Research,* vol. 34, no. 2, pp. 152-163, 2010.

[13] D. D. Domenico, A. Stefanopoulou, and G. Fiengo, "Lithium-ion battery state of charge and critical surface charge estimation using an electrochemical model-based extended Kalman filter," *Journal of dynamic systems, measurement, and control,* vol. 132, no. 6, pp. 061302, 2010.

[14] M. F. Samadi, S. M. Alavi, and M. Saif, "An electrochemical model-based particle filter approach for Lithium-ion battery estimation," in *IEEE 51st Annual Conference on Decision and Control (CDC)*, pp. 3074-3079, 2012.

[15] R. Klein, N. A. Chaturvedi, J. Christensen, J. Ahmed, R. Findeisen, A. Kojic, "Electrochemical Model Based Observer Design for a Lithium-Ion Battery," *IEEE Transactions on Control Systems Technology*, vol. 21, no. 2, pp. 289-301, 2013.

[16] M. Doyle, T. F. Fuller, and J. Newman, "Modeling of galvanostatic charge and discharge of the lithium/polymer/insertion cell," *Journal of the Electrochemical Society,* vol. 140, no. 6, pp. 1526-1533, 1993.

[17] T. F. Fuller, M. Doyle, and J. Newman, "Simulation and optimization of the dual lithium ion insertion cell," *Journal of the Electrochemical Society*, vol. 141, no. 1, pp. 1-10, 1994.

[18] H. J. Marquez, *Nonlinear control systems*. John Wiley, 2003.

[19] S. P. Boyd, *Linear matrix inequalities in system and control theory*. Vol. 15, Siam, 1994.

[20] A. Johansson, and A. Medvedev, "An observer for systems with nonlinear output map," *Automatica,* vol. 39, no. 5, pp. 909-918, 2003.

[21] K. Xiong, H.Y. Zhang, C.W. Chan, "Performance evaluation of UKF-based nonlinear filtering," *Automatica*, vol. 42, no. 2, pp. 261-270, 2006.

[22] X. Cao, and B. Ayalew, "Estimation and Predictive Control of Nonlinear Diffusion Processes with Application to Drying of Coatings," *Journal of Systems and Control Engineering*, in review, 2014.